S.-S. Li, Y.-W. Lin, Z. Ren, and C. T.-C. Nguyen, "A micromechanical parallel-class disk-array filter," *Proceedings*, 2006 IEEE Int. Frequency Control Symp., Geneva, Switzerland, May 29-June 1, 2007, pp. 1356-1361.

A Micromechanical Parallel-Class Disk-Array Filter

Sheng-Shian Li, Yu-Wei Lin, and Zeying Ren
Dept. of Electrical Engineering and Computer Science
University of Michigan
Ann Arbor, Michigan, USA
{ssli, ywlin, zyren}@umich.edu

Clark T.-C. Nguyen
Dept. of Electrical Engineering and Computer Sciences
University of California
Berkeley, California, USA
ctnguyen@eecs.berkeley.edu

***Abstract*—A method for realizing a high-order on-chip filter response that combines two fourth-order (i.e., two-pole) micromechanically-coupled MEMS-based disk-array sub-filters in a parallel configuration has been used to demonstrate a 163-MHz eighth-order (i.e., four-pole) bandpass filter with a 0.16%-bandwidth insertion loss of 2.73 dB, a 20 dB shape factor of only 1.78, and a termination impedance of only 4 kΩ, which is considerably smaller (i.e., better) than that achievable by a parallel combination of single disk resonators. The key to achieving such performance is the use of two capacitively-transduced disk-array composite sub-filters instead of the usual two stand-alone resonators used in previous parallel filter renditions. Here, the use of 275 μm × 360 μm sub-filters, each comprised of coupled radial-contour mode disk arrays, allows a combining of in-phase outputs to substantially raise output currents towards a 50× reduction in motional impedance versus that of a single disk resonator under the same operating conditions. This then lowers the termination impedance required by the overall filter, facilitating the ease with which other components can match to it, and thereby alleviating one of the primary drawbacks of capacitively-transduced micromechanical filters. By utilizing more than 128 disks and mechanical links, the 560 μm × 360 μm filter of this work comprises a true medium-scale integrated (MSI) mechanical circuit on a chip.**

I. Introduction

To date, on-chip mechanical filters comprised of several micromechanical resonators, coupled either mechanically via soft mechanical springs [1]; or electrically, using parallel-resonator architectures [2], ladder networks [3], or coupling capacitors [4]; have been demonstrated with impressive frequency characteristics. However, the recent desire for new RF front-end architectures capable of selecting channels right at RF [5], immediately after the antenna, now fuels a need for filters with tiny percent bandwidths and improved filter shape factor, i.e., faster passband-to-stopband roll-offs, to improve rejection of very close proximity adjacent channel interferers. In one rendition, shown in Fig. 1, channel-select filters are placed side-by-side (physically and in frequency) in a large bank that covers the needed range of frequencies. Such a channel-select filter bank would provide a formidable and

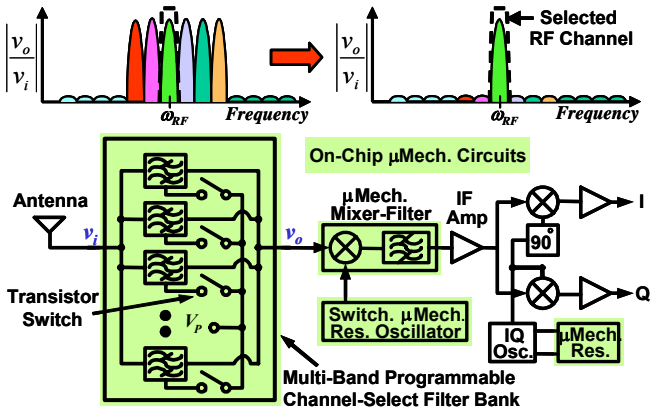

Fig. 1: Schematic block diagram for a MEMS-based receiver using a highly reconfigurable, low-power, channel-selector in its RF front-end. Here, the use of self-switching RF filters [5] in the channel selector obviates the need for lossy series switches. (Shaded blocks are micromechanical.)

unprecedented frequency processing capability if each filter in the bank were on/off switchable individually and simultaneously, since this would allow digital tunability of both center frequency and bandwidth. A method for improving filter shape factor when combining side-by-side filter responses would be a very welcome bonus.

Pursuant to achieving enhanced filter performance when combining digitally tunable channels and bandwidths, this work introduces a parallel-type filter architecture that combines the responses of two fourth-order series coupled filters to generate a higher-order filter response without the need for high-order mechanical coupling of resonant tanks. This design technique not only realizes digitally tunable channels and bandwidths, but also reduces the needed filter termination impedance from that otherwise required by an equivalent series coupled filter, and increases its power handling capability via a method similar to the array composite strategy of [6]. In combining series-coupled-resonator filters into parallel networks, this work provides a hybrid electrical and mechanical hierarchical circuit building block solution to attaining the smaller (i.e., better) filter shape factor and lower termination resistance required by the RF channel-selectors targeted by future wireless architectures.

This work was supported by DARPA and an NSF ERC in Wireless Integrated Microsystems.

S.-S. Li, Y.-W. Lin, Z. Ren, and C. T.-C. Nguyen, "A micromechanical parallel-class disk-array filter," *Proceedings*, 2006 IEEE Int. Frequency Control Symp., Geneva, Switzerland, May 29-June 1, 2007, pp. 1356-1361.

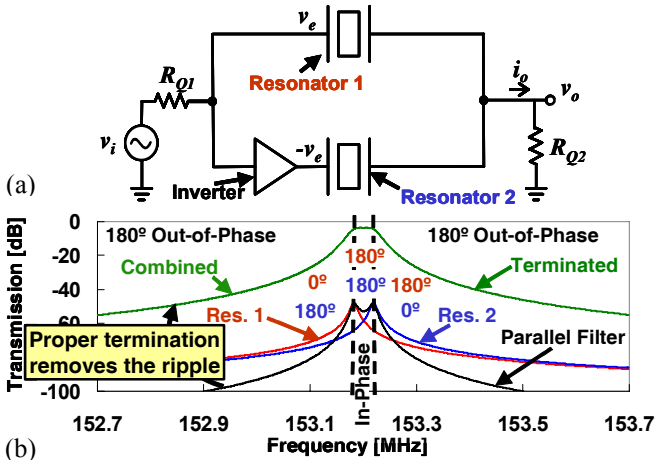

Fig. 2: (a) Schematic of a parallel-class filter using two standalone resonators. (b) Principle behind a parallel filter using two second-order resonators.

II. Filter Structure and Operation

The principle of operation in this work derives from the parallel-resonator filter concept of [2], where the properly spaced and phased frequencies of two resonators are combined to yield a flat passband and sharper roll-offs to the stopband. Fig. 2 illustrates the basic concept behind the parallel class filters used in a previous micromechanical filter demonstration [2]. Here, the inputs and outputs of two resonators are hooked together in a parallel configuration with an inverter or phase shifter in the second resonator's signal path to alter its relative phase from that of the first resonator. In Fig. 2, both resonators contribute second order transfer functions, each displaced from one another by a designed frequency separation, governed by the needed bandwidth. As depicted by the "combined" curve in the figure, frequency components between the resonant peaks add in-phase, while those outside this range subtract, resulting in a flatter passband between the peaks, increased rejection outside this range, and sharper roll-offs from the passband to stopband. Proper filter termination (via the R_Q's) then flattens the passband further to the desired amount of ripple. The end result:

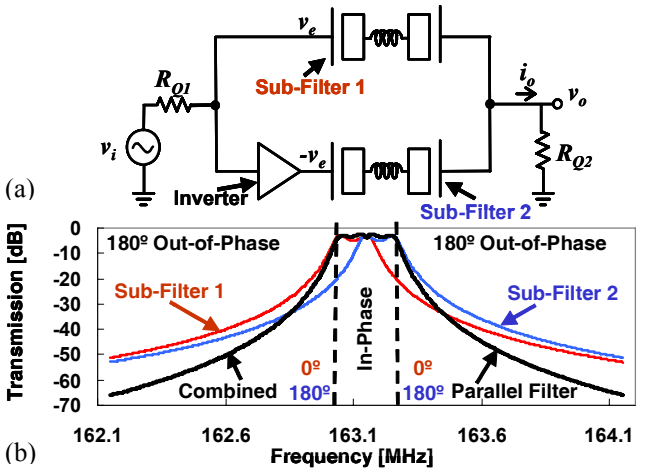

Fig. 3: (a) Schematic of a parallel-class filter using two sub-filters. (b) Principle behind an eighth-order parallel filter using two fourth-order sub-filters.

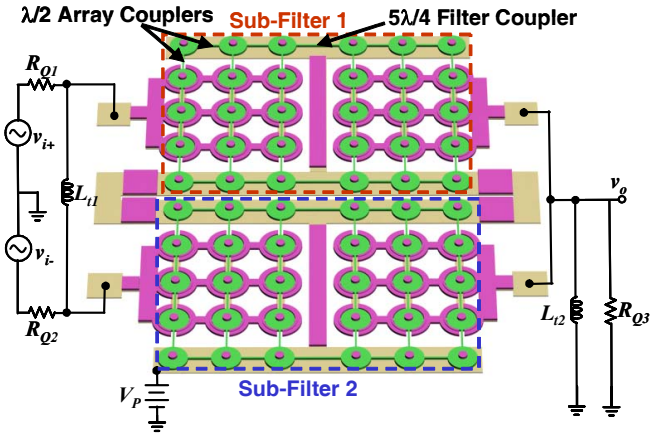

Fig. 4: Perspective-view schematic of the eighth-order micromechanical parallel-class disk-array filter implemented in this work.

A two-pole filter response formed via the combination of the outputs of single-pole resonator biquads.

A. Parallel-Coupled Sub-Filter Concept

This work goes one step further by replacing the previous resonators [2] with series-coupled sub-filter structures possessing higher order frequency transfer functions that then make possible even sharper roll-offs from passband to stopband and larger stopband rejections. Fig. 3(a) presents the circuit schematic for one embodiment of this approach, where two sub-filters with central frequencies f_{o1} and f_{o2} are driven by ac input voltage signals of opposite polarity, v_e and $-v_e$, and their output currents are summed, resulting in the output spectrum shown in Fig. 3(b). Similar to the previous case, both sub-filters contribute fourth-order transfer functions to the total frequency characteristic, each with different center frequencies spaced apart by a desired amount. As seen in Fig. 3(b), inputs at frequencies between the passbands of the two sub-filters produce output currents that are generally in phase, and thus add, creating a passband in this frequency range that is flat when the Q's of these filters are set to the right value via the (termination) resistive loads of Fig. 3(a). Those at frequencies outside this interval produce output currents that are out of phase, and thus subtract to provide more stopband rejection, as well as a shaper roll-off to the stopband. The bandwidth of the filter can be adjusted to a desired value by controlling the frequency separation (f_{o2} - f_{o1}) and the Q of the constituent filters. The overall parallel filter structure effectively combines two two-pole fourth-order sub-filters to yield a four-pole eighth-order overall filter response with sharper roll-offs and larger stopband rejections.

B. Physical Parallel Filter Implementation

Fig. 4 presents the perspective-view schematic of the actual implementation of the parallel-class disk-array filter in this work, where each two-pole sub-filter structure utilizes two large disk-array composites, each of which contains 15 contour-mode disk resonators mutually linked by λ/2 longitudinal mode coupling beams [7] to accentuate a single resonator response in which all λ/2-connected disks vibrate at exactly the same frequency. To expand upon this, the coupled

multiple resonator mechanical system of each disk-array composite has many modes of vibration, with only one of them desired for filtering. To control the modes so that only the desired one is visible, while the undesired ones suppressed, the coupling scheme for each disk-array is wavelength optimized, as first described in [8][9]. In the scheme of Fig. 4, half-wavelength (i.e., λ/2) extensional-mode coupling beams are used to drive all the modes ideally infinitely apart in the frequency domain, allowing the mode selected by the input excitation electrode configuration to be all alone, hence the only one appearing. The fully surrounding electrode configuration used for all disks in the composite arrays of Fig. 4 essentially forces in-phase motion of the disks in each individual array.

Among the 15 disks in each disk-array composite resonator, 9 disks surrounded by electrodes operate as electromechanical converters that transfer energy between the electrical and mechanical domains. Because all disks vibrate in-phase at exactly the same frequency, the currents of all 9 of these disks can be summed to achieve a 9× higher total current over that of a single disk resonator, which then reduces the motional resistance by 9× and raises the power handling capability by this same factor. Of the remaining 6 disks, the 3 at the outside edges of the circuit structure supply bias voltages for the whole filter structure, while the 3 on the inside comprise "buffering" disks (to be described more fully) that shield the disk-array composite from mechanical interconnections to neighboring resonators.

Both composite arrays in the top sub-filter are identical with center frequency f_{o1}, as are both composite arrays in the bottom sub-filter, centered at f_{o2}. To effect a splitting of the composite-array center frequencies into two mode frequencies that define the passband of each sub-filter, the energy from each composite-array in a given sub-filter is coupled to that in the other via extensional mode beams dimensioned to correspond to an odd multiple (in this case, n=5) of a quarter-wavelength (e.g, $n\lambda/4$). Instead of directly attaching the coupling beams to the electrically-driven composite array resonators, as done in previous micromechanical filters [1][6], this work connects them through the aforementioned mechanical buffering disks, which help to maintain a mechanical symmetry that suppresses the incidence of unwanted spurious modes [7]. For each sub-filter, connecting the array-composites in this manner yields a fourth-order (i.e., two-pole) filter response that, due to summing in the arrays, exhibits a much smaller device impedance and higher power handing capability than would a filter using single resonators, such as that of [2].

The overall filter structure uses a total of 128 combined resonators and links to effect one of the largest micromechanical circuits achieved to date. In addition, its design constitutes an example of true hierarchical mechanical circuit design, where each identical disk resonator makes up the first level of hierarchy; each array composite, the second; and the filter coupling interconnects (aided by the bias and buffering disks), the third. Needless to say, as they did with transistor integrated circuits, hierarchical design approaches will likely be instrumental to attaining eventual LSI and VLSI mechanical circuits with unprecedented functionality.

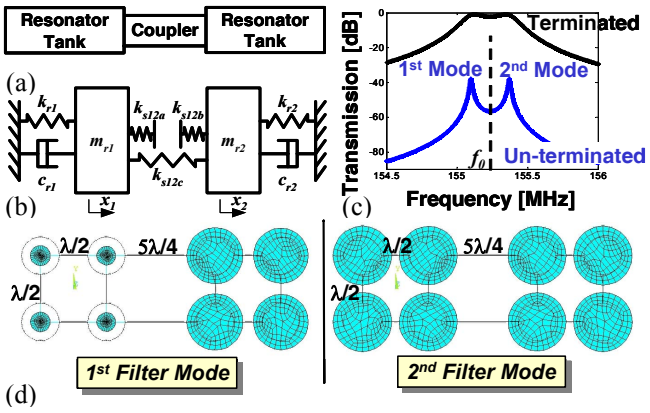

Fig. 5: Disk sub-filter modeling. (a) Basic topology; (b) equivalent lumped parameter mechanical model; (c) un-terminated and terminated frequency characteristics; and (d) simplified finite element simulated mode shapes, including out-of-phase and in-phase filter modes for each micromechanical disk-array sub-filter.

III. Equivalent Circuit Modeling

Using the aforementioned scheme, where judicious choice of half and quarter-wavelength couplers at specific locations are used to effect in-phase motions that group together the coupled disk constellations into what are essentially composite devices, the whole complicated mechanical system of each disk-array sub-filter in Fig. 4 condenses to two resonator tanks coupled together as shown in Fig. 5(a). This structure can in turn be modeled via the lumped parameter mass-spring-damper mechanical circuit of Fig. 5(b), which generates the un-terminated frequency characteristic shown in Fig. 5(c). After proper filter termination, the jagged passband is flattened into the ideal filter passband, also shown in Fig. 5(c). Each peak in this spectrum corresponds to a specific mechanically vibrating mode shape. In the left side of Fig. 5(d), the input and output disk arrays vibrate out-of-phase, creating the least stress in the 5λ/4 couplers, thereby resulting in the low frequency peak of Fig. 5(c). On the other hand, the second filter mode, shown to the right, exhibits in-phase motion between the input and output disk-arrays. Here,

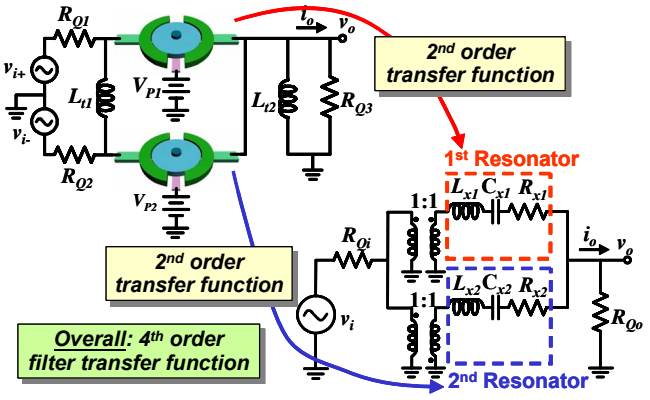

Fig. 6: Equivalent electrical circuit of the parallel filter using stand-alone disk resonators.

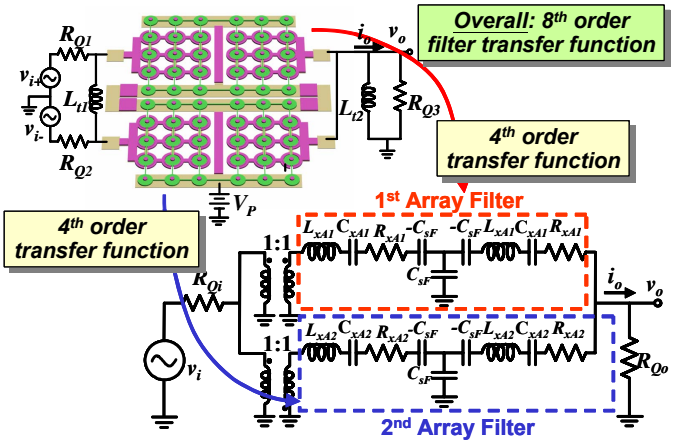

Fig. 7: Equivalent electrical circuit of the parallel filter using sub-filters comprising disk-array composites.

the couplers are now stressed, which raises the overall stiffness of the system, thereby achieving a higher frequency mode. The two modes combine to yield the filter passband of Fig. 5(c).

As has been done with previous series micromechanical filters, the electrical equivalent circuit for this parallel filter can be specified via electromechanical analogy. In the parallel filter comprised of single resonators in Fig. 6, each resonator comprises a mass-spring-damper system that can be modeled by an *LCR* circuit, providing a second order transfer function. The properly phased combination of these *LCR*'s in the parallel configuration of Fig. 6 then yields a fourth order frequency characteristic.

On the other hand, in the parallel filter using series-coupled disk-array sub-filters shown in Fig. 7, each sub-filter is now modeled by two *LCR* circuits, each of which represents a disk array composite, coupled by a T-network of capacitors. The T-network of capacitors is appropriate because the filter coupling beams are actually mechanical transmission lines, so like electrical transmission lines, can be represented by a T-network of energy storage elements, in this case capacitors. Clearly, from the equivalent circuit of Fig. 7, each sub-filter contributes a fourth order transfer function with different center frequencies. When hooked into the parallel topology shown in the figure, the overall system yields an eighth order frequency characteristic, capable of attaining

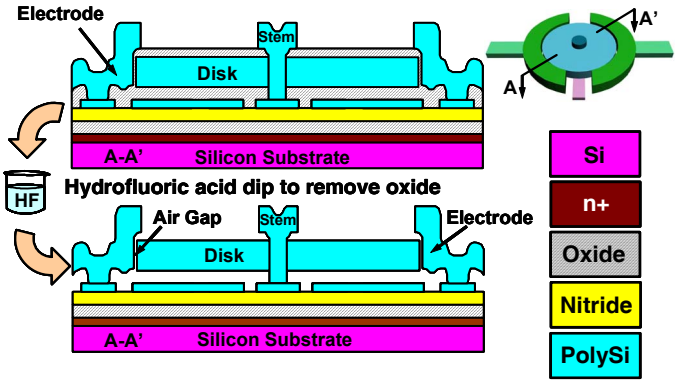

Fig. 8: Cross-sections of the last few steps in the small-lateral-gap, self-aligned-stem, wafer-level fabrication process used.

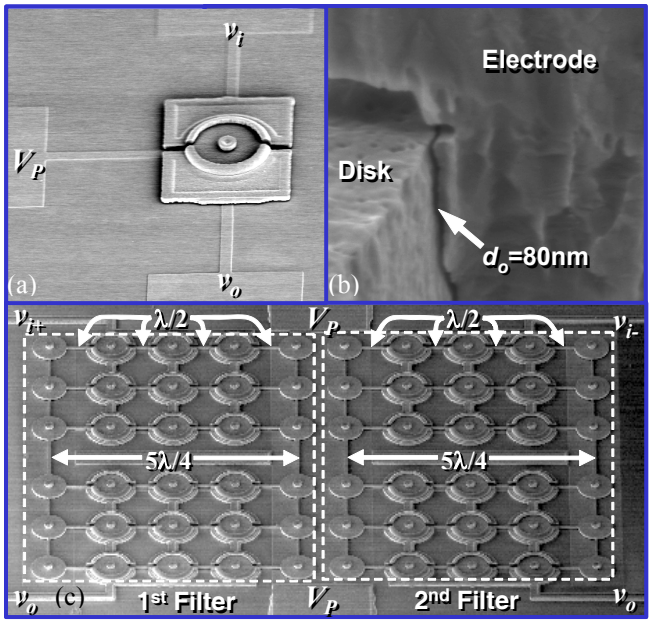

Fig. 9: SEM's of devices achieved via the process of Fig. 8: (a) Stand-alone disk, (b) zoom-in on the electrode-to-resonator gap, and (c) two sub-filters comprising a disk-array parallel filter.

larger stopband rejection and a faster roll-off from passband to stopband.

IV. Fabrication and Experimental Results

The parallel filter of this work was fabricated using a surface micromachining fabrication sequence similar to that described in [10], which uses two polysilicon depositions to effect self-alignment of resonant structures to their supports and a sacrificial sidewall spacer to define lateral electrode-to-resonator gaps on the order of 80 nm. Fig. 8 presents cross-section views of the last few steps of the fabrication process. Here, several thin films deposited and patterned on the silicon substrate form the structure at the top of Fig. 8, where the disk to be suspended is temporarily supported by a sacrificial oxide layer during its own deposition and patterning, and an 80 nm sidewall sacrificial oxide film is used as a temporary gap material that defines the electrode-to-resonator gap spacing. After a hydrofluoric acid release step, all sacrificial oxides are removed and the resonator is free to vibrate as shown in the lower view of Fig. 8. Fig. 9 presents SEM's of structures resulting from this process, including (a) a stand-alone disk resonator; (b) a zoom-in view on its 80 nm electrode-to-resonator gap; and (c) two disk-array sub-filters in close proximity used to realize high-order parallel-class filters that verify the design methods described herein. When self-aligned to their stems [10], micromechanical disks regularly achieve *Q*'s greater than 10,000, which greatly reduces the insertion loss of filters comprised of these high-*Q* resonators. It should be noted that the successful demonstration reported here of micromechanical circuits with the level of complexity depicted in Fig. 9(c) testifies to the high yield of the fabrication process used.

For comparative purposes, parallel filters using stand-alone disks (as opposed to array-composite sub-filters) were

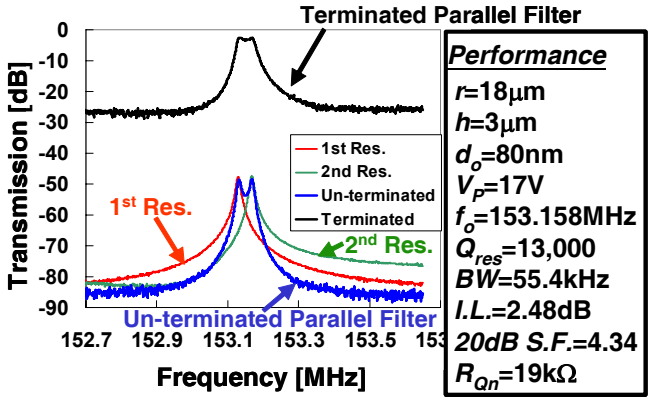

Fig. 10: Frequency characteristics for a fabricated micromechanical parallel-resonator filter centered at 153.16 MHz, explicitly showing how the frequency characteristics of its constituent disk resonators combine.

tested first. Fig. 10 presents the un-terminated and terminated frequency characteristics of a parallel-resonator filter response formed by properly-phased summation of the responses of two Fig. 9(a)-type constituent resonators. The bottom curves correspond to the un-terminated case and clearly show the in-band addition and out-of-band subtraction of the individual resonator frequency characteristics to form the un-terminated filter characteristic. The addition of proper 19 kΩ filter terminations then yields the curve at the top of Fig. 10, which constitutes the frequency characteristic of the desired parallel-resonator filter centered at 153.2 MHz with an insertion loss of only 2.48 dB for a channel-select-like 0.036% bandwidth. The passband ripple is smaller than 0.5 dB, and the 20 dB filter shape factor is 4.34. The need for termination resistors as large as 19 kΩ derives from the use of only single capacitively-transduced disk resonators, each of which have high motional resistance.

To lower impedances and attain better filter performance, parallel filters utilizing disk-array composite sub-filters were tested next. Fig. 11 presents the un-terminated frequency characteristics of such a parallel-class filter using the two sub-filters of Fig. 9(c) instead of single resonators to achieve a filter shape factor and stopband rejection clearly better than that seen in Fig. 10. Ignoring for now the spurious modes seen right above the desired passband, the curves in Fig. 11

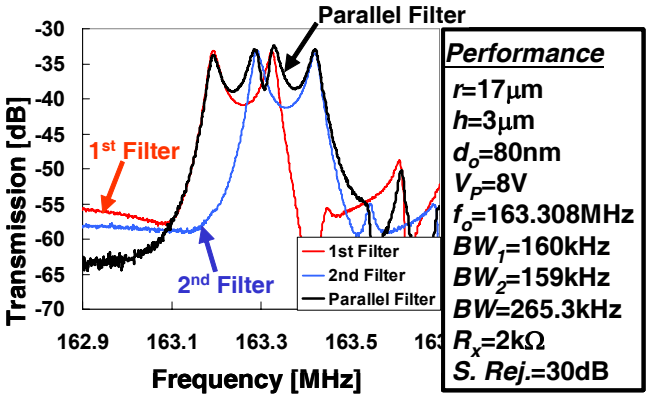

Fig. 11: Frequency characteristics for a fabricated 8th-order micromechanical parallel disk-array filter, explicitly showing how the frequency characteristics of its constituent 4th-order sub-filters combine.

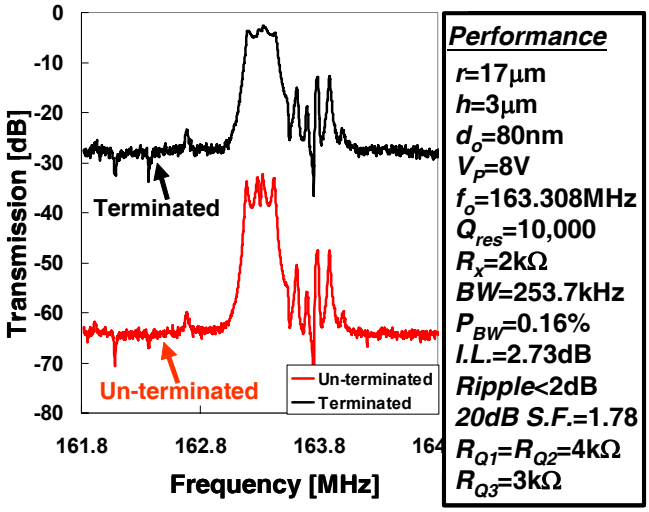

Fig. 12: Un-terminated and terminated spectra for a fabricated 8th-order micromechanical parallel-class disk-array filter.

clearly demonstrate in-band addition and out-of-band subtraction that reduce the combined passband ripple from that of each sub-filter, while expanding the filter bandwidth and increasing the stopband rejection. The spurious modes seen above the passband are a result of two implementation deficiencies: first, the resonance frequencies of the disks turned out to be 8 MHz higher than the designed frequency, so the array coupling beams designed to be λ/2 couplers at the design frequency are no longer λ/2 at the actual frequency; second, the sub-filter structures utilized in this work are single-ended, so do not benefit from the spurious mode cancelling actions of balanced designs that employ λ coupling to effect a differential operation mode [11]. If the sub-filters of this work were designed to be differential, like those of [11], the spurious modes would be much less problematic.

The termination resistance required for a parallel filter like that of Fig. 4 is governed only by the needs of its sub-filters, and is thereby independent of the combined filter bandwidth. Thus, from the standpoint of attaining wider bandwidth, the parallel filter concept described herein provides a distinct advantage over series coupled filters in that wider bandwidth can be achieved without the need to increase the termination resistance over that required by its sub-filters.

Fig. 12 finally presents the terminated frequency characteristic for the 163.3-MHz, 0.16% bandwidth parallel-class disk-array filter, using termination resistors of only 4 kΩ for a dc-bias voltage of 8V, and showing a low insertion loss of only 2.73 dB with passband ripple less than 2 dB. The 20 dB shape factor is 1.78, which is impressive and much smaller than that of the parallel-resonator filter of Fig. 10.

V. Fitler Bank With Switchable Frequency and Bandwidth

With such a small insertion loss for such a tiny bandwidth, filters like that demonstrated in Fig. 12 now encourage the implementation of channel-select filter banks that might soon transform the design of future wireless transceivers [5].

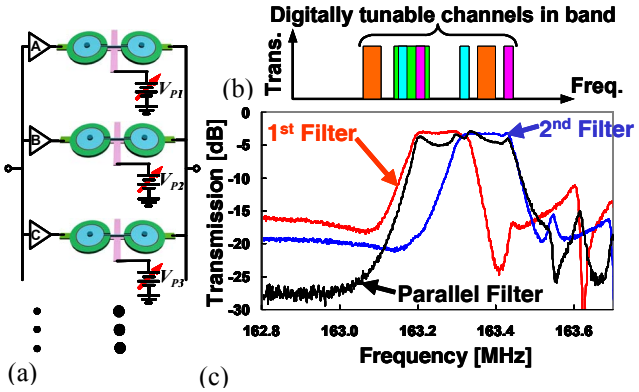

Fig. 13: (a) Functional schematic of an RF channel-select filter bank employing the parallel configuration of this work to realize (b) digitally tunable channels for the future wireless systems. (c) Implementation of the functions in (b) via the parallel filter of Fig. 4

The filters of this work are especially useful for channel-selection, since their use of capacitive transducers allow them to be switched on and off by merely adjusting the dc bias voltage from V_P to zero, as shown in Fig. 13(a). This obviates the need for RF MEMS switches, which then reduces cost, and eliminates a potential reliability concern. In addition to center frequency switching, the parallel filter concept of this work makes possible the additional benefit of bandwidth switching, where the bandwidths of two (or more) filters in the bank can now be combined to yield a digitally tunable bandwidth. With this ability, the choice of center frequency-bandwidth combinations widens considerably, as shown in Fig. 13(b), where several frequency-bandwidth combinations are turned on simultaneously.

As a simple example of how the parallel filter of this work can accomplish digital tuning/switching of frequencies and bandwidths, if only V_{P1} is on in Fig. 13(a), with all others set to zero (or floating in some renditions), the lower frequency channel (i.e., the red line) in the frequency spectrum of Fig. 13(c) ensues. If the second channel (i.e., blue line) is then required, one can simply turn on V_{P2} and turn off V_{P1}—i.e., set it to zero. If a larger bandwidth is needed, the wider channel (i.e., black line) can be conveniently realized by combining the responses of the two individual filters via the parallel configuration described herein.

VI. Conclusion

A method for realizing a high-order on-chip filter response that combines two series-coupled micromechanical disk-array sub-filters in a parallel configuration has been used to demonstrate a 163-MHz eighth-order bandpass filter with a 0.16%-bandwidth insertion loss of 2.73 dB, a 20 dB shape factor of only 1.78, and a termination impedance of only 4 kΩ. The key to achieving such performance is the use of two capacitively-transduced disk array-composite sub-filters instead of the usual two stand-alone resonators used in previous parallel filter renditions. By utilizing more than 128 disks and mechanical links, the 560 μm x 360 μm filter comprises a true medium-scale integrated (MSI) mechanical circuit on a chip. In addition, programmable channels and bandwidths adjustable via device dc-bias voltages were also demonstrated, in a topology expected to greatly benefit the design of future wireless front-ends, such as those for cognitive radio. Perhaps even more significant than sheer performance, however, is the demonstration via this work that mechanical circuit design methodologies can be just as powerful as those used in the transistor world to enhance functionality via a hierarchical building block approach.

Acknowledgment

This work was supported by DARPA and an NSF ERC in Wireless Integrated Microsystems.

References

[1] F. D. Bannon III, J. R. Clark, and C. T.-C. Nguyen, "High-*Q* HF microelectromechanical filters," *IEEE Journal of Solid-State Circuits*, vol. 35, no. 4, pp. 512-526, April 2000.

[2] J. R. Clark, A.-C. Wong, and C. T.-C. Nguyen, "Parallel-resonator HF Micromechanical Bandpass Filters," *Digest of Technical Papers*, 1997 International Conference on Solid-State Sensors and Actuators, Chicago, Illinois, June 16-19, 1997, pp. 1161-1164.

[3] G. Piazza, P. J. Stephanou, M. B. J. Wijesundara, and A.P. Pisano, "Single-chip multiple-frequency filers based on contour-mode aluminum nitride piezoelectric micromechanical resonators," *Dig. of Tech. Papers*, the 13th Int. Conf. on Solid-State Sensors & Actuators (Transducers'05), Seoul, Korea, June 5-9, 2005, pp. 2065-2068.

[4] S. Pourkamali, R. Abdolvand, F. Ayazi, "A 600 kHz electrically-coupled MEMS bandpass filter," *Proceedings*, 16th International IEEE Micro Electro Mechanical Systems Conference (MEMS '03), Kyoto, Japan, Jan. 19-23, 2003, pp. 702-705.

[5] C. T.-C. Nguyen, "Vibrating RF MEMS overview: applications to wireless communications," *Proceedings*, Photonics West: MOEMS-MEMS 2005, San Jose, California, Jan. 22-27, 2005, Paper No. 5715-201.

[6] M. U. Demirci and C. T.-C. Nguyen, "A low impedance VHF micromechanical filter using coupled-array composite resonators," *Dig. of Tech. Papers*, the 13th Int. Conf. on Solid-State Sensors & Actuators (Transducers'05), Seoul, Korea, June 5-9, 2005, pp. 2131-2134.

[7] S.-S. Li, Y.-W. Lin, Z. Ren, and C. T.-C. Nguyen, "Disk-array design for suppression of unwanted modes in micromechanical composite-array filters," *Tech. Digest*, 19th IEEE Int. Conf. on Micro Electro Mechanical Systems (MEMS'06), Istanbul, Turkey, Jan. 22-26, 2006, pp. 866-869.

[8] Y.-W. Lin, S.-S. Li, Z. Ren, and C. T.-C. Nguyen, "Low phase noise array-composite micromechanical wine-glass disk oscillator," *Technical Digest*, IEEE Int. Electron Devices Mtg., Washington, DC, Dec. 5-7, 2005, pp. 287-290.

[9] Y.-W. Lin, L.-W. Hung, Y. Lin, S.-S. Li, and C. T.-C. Nguyen, "Quality factor boosting via mechanically-coupled arraying," *Dig. of Tech. Papers*, the 14th Int. Conf. on Solid-State Sensors & Actuators (Transducers'07), Lyon, France, June 10-14, 2007, pp. 2453-2456.

[10] J. Wang, Z. Ren, and C. T.-C. Nguyen, "1.156-GHz self-aligned vibrating micromechanical disk resonator," *IEEE Transactions on Ultrasonics, Ferroelectrics, and Frequency Control*, vol. 51, no. 12, pp. 1607-1628, Dec. 2004.

[11] S.-S. Li, Y.-W. Lin, Z. Ren, and C. T.-C. Nguyen, "An MSI micromechanical differential disk-array filter," *Dig. of Tech. Papers*, the 14th Int. Conf. on Solid-State Sensors & Actuators (Transducers'07), Lyon, France, June 10-14, 2007, pp. 307-311.